Toward understanding the S2-S3 transition in the Kok cycle of Photosystem II

Amin, Muhamed; Kaur, Divya; Gunner, M. R.; Brudvig, Gary W.

Published in:
Inorganic Chemistry Communications

DOI:
10.1016/j.inoche.2021.108890

Publication date:
2021

Inorganic Chemistry Communications 133 (2021) 108890

Contents lists available at ScienceDirect

Inorganic Chemistry Communications

journal homepage: www.elsevier.com/locate/inoche

Toward understanding the S_2-S_3 transition in the Kok cycle of Photosystem II: Lessons from Sr-substituted structure

Muhamed Amin [a,b], Divya Kaur [c,d,e], M.R. Gunner [d,e], Gary Brudvig [f]

[a] Rijksuniversiteit Groningen Biomolecular Sciences and Biotechnology Institute, University of Groningen, Groningen, Netherlands
[b] Science Department, University College Groningen, University of Groningen, Groningen, Netherlands
[c] Department of Chemistry, Brock University, 500 Glenridge Avenue, St. Catharines, ON L2S 3A1, Canada
[d] Department of Chemistry, The Graduate Center of the City University of New York, New York, NY 10016, United States
[e] Department of Physics, City College of New York, New York, NY 10031, United States
[f] Department of Chemistry, Yale University, New Haven, CT 06520-8107, United States

ARTICLE INFO

Keywords:
Photosystem II
Density functional theory
Continuum electrostatics

ABSTRACT

Understanding the water oxidation mechanism in Photosystem II (PSII) stimulates the design of biomimetic artificial systems that can convert solar energy into hydrogen fuel efficiently. The Sr^{2+}-substituted PSII is active but slower than with the native Ca^{2+} containing PSII as an oxygen evolving catalyst. Here, we use Density Functional Theory (DFT) to compare the energetics of the S_2 to S_3 transition in the $Mn_4O_5Ca^{2+}$ and $Mn_4O_5Sr^{2+}$ clusters. The calculations show that deprotonation of the water bound to Ca^{2+} (W3), required for the S_2 to S_3 transition, is energetically more favorable in $Mn_4O_5Ca^{2+}$ than $Mn_4O_5Sr^{2+}$. In addition, we have calculated the pK_a of the water that bridges Mn4 and the Ca^{2+}/Sr^{2+} in the S_2 state using continuum electrostatics. The calculations show that the pK_a is higher by 4 pH units in the $Mn_4O_5Sr^{2+}$cluster.

The oxygen evolving complex (OEC) is a unique natural bioinorganic cluster that catalyzes the water oxidation reaction in the 5-step (S_0, S_1, S_2, S_3, S_4) Kok cycle [1,2]. The core of the OEC contains a metal cluster of four Mn and one Ca^{2+} connected through bridging oxygens [2–4]. Ca^{2+} depletion [5,6] blocks the S_2-S_3 transition, while replacing Ca^{2+} with Sr^{2+} reduces the catalytic activity [7–10]. In addition, in the absence of Ca^{2+}, electron transfer from the OEC to Tyrosine (Y_Z) becomes uphill [11].

Calcium and strontium belong to group 2 alkaline earth metals in the periodic table. Thus, they are chemically similar and have a stable oxidation state of +2. However, Ca^{2+} is a stronger Lewis acid, which indicates that aqua-Ca^{2+} compounds have a lower pK_a than aqua-Sr^{2+} (measured pK_a is 2 pH unit lower). This difference in proton affinity of the bound waters may be the reason for the difference in the catalytic activity in the Sr-substituted PSII [10,12,13]. Here, we use Density Functional Theory (DFT) to compare the energetics of the S_2-S_3 transition in native and Sr-substituted PSII.

The S_2-S_3 transition involves the insertion of a water molecule that binds to the OEC complex. Different mechanisms such as the pivot and carousal mechanisms have been proposed for water insertion [14,15]. The transition also depends on the specific S_2 spin state involved in the transition to the S_3 state. The S_2 state has two types of EPR signals: multiline which corresponds to g = 2 and broad corresponding to g = 4.1 or higher depending upon the species and experimental conditions [16,17]. In the g = 4.1 EPR state, Mn1, Mn2, and Mn3 are in the IV oxidation state, while Mn4 is in the III state (Fig. 1) [18]. In the g = 2 redox isomer, Mn1 is Mn(III) while Mn4 is Mn(IV). However, the two S_2 spin states can interconvert [17–19].

Recent computational studies proposed different models for the S_2 spin states, which differ in either the protonation states of W1 and W2 of Mn4 or the protonation states of the oxygen bridges mainly O4 [20–22]. An open question is: Which spin and protonation states of the S_2 state are oxidized to the S_3 state? Different mechanisms have been proposed. For instance, experimental studies [16] including temperature dependence kinetics experiments and computational studies including those using DFT and continuum electrostatics based methods [23–25] have proposed that conversion of the S_2 g = 2 open cubane to the g = 4.1 closed cubane occurs before OEC oxidation to the S_3 state. The model used for both g = 2 and g = 4.1 spin isomers involves a deprotonated oxygen bridge O4. Another DFT study proposed the transition from a high spin open cubane S_2 state with O4 deprotonated to the S_3 state [26]. Recent studies using broken symmetry DFT and spin ladder calculations show that the g = 4.8/4.9 form observed at high pH corresponds to the high spin S = 7/2 species involved in the advancement to S_3. This model of

E-mail address: m.a.a.amin@rug.nl (M. Amin).

https://doi.org/10.1016/j.inoche.2021.108890
Received 21 May 2021; Received in revised form 27 August 2021; Accepted 29 August 2021
Available online 1 September 2021

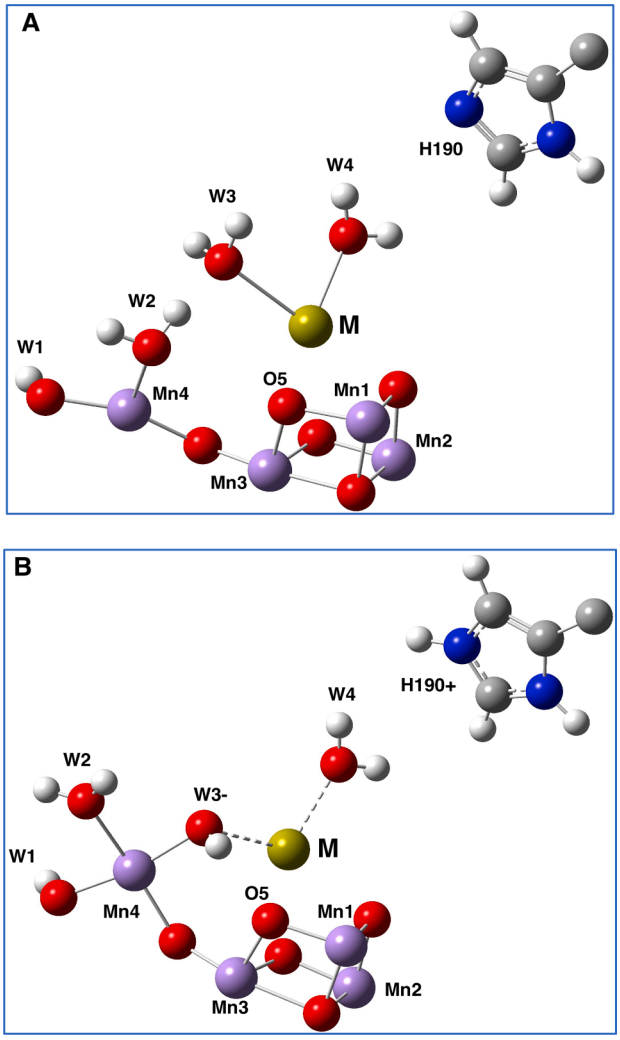

Fig. 1. **A** represents the S_2 state with HIS190 neutral. **B** represents the S_2 state with $HIS190^+$ protonated. **M** is Ca^{2+} or Sr^{2+}. Mn1, Mn2, Mn3 are in the IV oxidation state. Mn4 is III. The complete description of the model is included in the supplementary information.

the S_2 state proposes a proton shift where O4 is protonated and the water bound Mn4 W1 is a hydroxide [21,22]. Other studies involving time-resolved photothermal beam deflection measurements suggest that a proton is released from the OEC or surroundings when the nearby Tyr, Y_Z, is oxidized before Mn oxidation in the S_2-S_3 transition [27,28].

Based on our earlier classical electrostatic calculations and DFT study [23], we proposed that the S_2-S_3 transition starts with the transition from the g = 2 to g = 4.1 state followed by deprotonation of the W3 Ca^{2+} ligand [29]. This is coupled to the protonation of HIS190 upon the oxidation of the secondary donor Yz*. The deprotonated W3 moves toward Mn4 adding the sixth ligand to its coordination shell to facilitate its oxidation to the IV state. Similar mechanisms have been proposed by previous theoretical [30–33] and experimental [10] studies.

Here, we compare the energies of a proton shift between OEC cluster in the S_2 g = 4.1 state and His190 in both $Mn_4O_5Ca^{2+}$ and $Mn_4O_5Sr^{2+}$ clusters. In structure **A** HIS190 and W3 are neutral (Fig. 1A) and in **B** $HIS190^+$ is protonated and W3 is a OH^- bridge between Mn4 and Ca^{2+} (Fig. 1B). The structures were optimized at the DFT level using the B3LYP functional and 6-31G(d) basis sets for N, O, C and H atoms, while SDD basis sets are used for Mn, Ca and Sr. All the Mn ions are in the high spin state. Furthermore, the energies are compared using different levels of theory; B3LYP/6-31G+(d) and B97D/6-31G+(d) [34,35].

The energy differences between the **A** and **B** states ($\Delta G_{(B\text{-}A)}$) at different levels of theory are shown in Table 1. In general, the **B** state (protonated HIS190 and hydroxyl on W3) is always more favorable for the $Mn_4O_5Ca^{2+}$ than the $Mn_4O_5Sr^{2+}$ cluster. The large energy difference obtained for the $Mn_4O_5Sr^{2+}$ cluster using the B3LYP/6-31G(d) level of theory indicates the importance of including diffuse functions in the basis sets when modeling large ions. These diffuse functions provide a flexible representation to the tail part of the atomic orbitals further from the nucleus [34,35].

Sr^{2+} is larger than Ca^{2+} by 0.1 Å, which elongates the interatomic distances between the Sr^{2+} and the rest of the atoms in the Mn cluster. This is seen in the optimized structures of the **A** and **B** states with Ca^{2+} and Sr^{2+} clusters (Table 2). In addition, the dispersion interaction between the metal and the water ligand is expected to push the water away in case of Sr^{2+}, which will result in smaller electrostatic interactions and a higher pK_a. This is found for aqua-Ca^{2+} and aqua-Sr^{2+} compounds, where the water bound to Sr^{2+} has a higher pK_a than those bound to Ca^{2+}. Thus, the Sr^{2+} structure is more stable with neutral W3 (Fig. 1A). However, with Ca^{2+}, W3 deprotonates forming a hydroxide that moves to bridge Mn4 and Ca^{2+} (Fig. 1B).

The optimized DFT structures show that Mn-Sr^{2+} distances are in general longer than Mn-Ca^{2+}. In the **A** state the Sr^{2+}-W3(HOH) distance is 0.1 Å longer than Ca^{2+}-W3(HOH). In the **B** state the Sr^{2+}-$W3(OH)^-$ distance is 0.2 Å longer because Ca^{2+} moves significantly toward Mn4 after the deprotonation of W3. To further compare the $Mn_4O_5Ca^{2+}$ the $Mn_4O_5Sr^{2+}$clusters, we calculated the pK_a of W3 in the **A** state with HIS190 protonated for both clusters using Monte Carlo sampling with continuum electrostatics and molecular mechanics energies [36,37]. MCCE (Multi-Conformer Continuum Electrostatics) [37] is used to calculate the pK_a starting with the DFT optimized structure by calculating the difference in the free energies ΔΔG of the protonated and deprotonated conformers. The ΔΔG includes the electrostatics and the desolvation energies calculated using DELPHI [38] (see supporting information). The surroundings of the isolated DFT structure are given a dielectric constant of 80. Thus, the model removes long-range interactions from the protein. The high dielectric solvent around the isolated cluster decreases the pairwise electrostatic interactions within the cluster, which can be balanced by the solvent stabilizing the cluster charges.

W3 has a pK_a of 6.5 in the $Mn_4O_5Ca^{2+}$ and 10.3 in the $Mn_4O_5Sr^{2+}$ clusters. Because the Sr^{2+} has a larger ionic radius than Ca^{2+}, the optimized structures show that the W3 water ligand is closer to Ca^{2+}, Mn4 (III) and Mn1(IV) (Table 2), which explains the difference in proton affinity with Ca^{2+} or Sr^{2+} in the cluster. This is supported by the DFT calculations, which show that with Ca^{2+} **B** has a lower energy than **A** indicating an easier deprotonation of W3. The calculated pK_a of W3 is significantly lower than 14, the value obtained by Saito et al. [39,40]. However, the pK_a of W3 is expected to be lower than the aqua Ca^{2+} pK_a (~12) due to the positively charged Mn cluster. In addition, the nearby positively charged $HIS190^+$, favors the hydroxide conformer and reduces the pK_a of W3.

An open question is: what is the source of the proton which is released after Y_z is oxidized but before the OEC advances to the S_3 state [3,41]. As there are no protons bound to the bridging oxygens in the S_2 state, the donors are likely to be terminal water ligands bound to Mn4 [42,43] or to Ca^{2+} [44]. Previous studies have shown the Mn4-bound water W1 is deprotonated upon formation of the tyrosyl radical, however the proton is trapped by the nearby acceptor D61 in the S_2 state

Table 1
The $\Delta G_{(B\text{-}A)}$ DFT energies.

	B3LYP/6-31G(d)	B3LYP/6-31G+(d)	B97D/6-31G+(d)
$Mn_4O_5Ca^{2+}$	−2.3	−8.7	−6.8
$Mn_4O_5Sr^{2+}$	13.0	−8.0	−6.4

Energy differences are expressed in Kcal/mol. The transition from A to B state is more favorable in the $Mn_4O_5Ca^{2+}$ cluster than the $Mn_4O_5Sr^{2+}$

Table 2
Interatomic distances in A and B states.

	A		B	
	Ca^{2+}	Sr^{2+}	Ca^{2+}	Sr^{2+}
Mn1	2.50	3.58	3.49	3.67
Mn4	4.35	4.51	3.58	2.64
W3	2.55	2.66	2.39	2.58
W4	2.33	2.50	2.35	2.53
O5	2.66	2.78	2.66	2.77

All distances are reported in Å. In general, the interatomic distances are longer for Sr^{2+}.

[14,25,45–47].

The present study utilizes the S_2 g = 4.1 models for Ca^{2+} and Sr^{2+} containing PSII to understand the nature of deprotonation event. Our DFT calculations support the deprotonation of W3 in the S_2 to S_3 transition, which is also supported by the XFEL structures comparing the S_1, S_2 and S_3 states [48]. In conclusion, the above calculation shows that the S_2-S_3 transition occurs upon the loss of a proton from Ca-ligated W3 in the presence of $HIS190^+$ maintaining the hydrogen bonding network necessary for the proton transfer. In the Sr^{2+}-substituted structure, the energy barrier for deprotonating W3 is higher due to the weaker electrostatic interactions that enhance proton affinity.

CRediT authorship contribution statement

Muhamed Amin: Conceptualization, Methodology, Writing – original draft. **Divya Kaur:** Methodology, Writing – original draft. **M.R. Gunner:** Writing – review & editing. **Gary Brudvig:** Writing – review & editing.

Declaration of Competing Interest

The authors declare that they have no known competing financial interests or personal relationships that could have appeared to influence the work reported in this paper.

Acknowledgements

The authors acknowledge computational resources from the support by the U.S. Department of Energy, Office of Science, Office of Basic Energy Sciences, Division of Chemical Sciences, Geosciences, and Biosciences via Grants DESC0001423 (M.R.G. and V.S.B.), and DE-FG02-05ER15646 (G.W.B.).

Appendix A. Supplementary material

Supplementary data to this article can be found online at https://doi.org/10.1016/j.inoche.2021.108890.

References:

[1] D.J. Vinyard, G.W. Brudvig, Progress toward a Molecular Mechanism of Water Oxidation in Photosystem II, Annu. Rev. Phys. Chem. 68 (1) (2017) 101–116, https://doi.org/10.1146/annurev-physchem-052516-044820.
[2] J. Kern, R. Chatterjee, I.D. Young, F.D. Fuller, L. Lassalle, M. Ibrahim, S. Gul, T. Fransson, A.S. Brewster, R. Alonso-Mori, R. Hussein, M. Zhang, L. Douthit, C. de Lichtenberg, M.H. Cheah, D. Shevela, J. Wersig, I. Seuffert, D. Sokaras, E. Pastor, C. Weninger, T. Kroll, R.G. Sierra, P. Aller, A. Butryn, A.M. Orville, M. Liang, A. Batyuk, J.E. Koglin, S. Carbajo, S. Boutet, N.W. Moriarty, J.M. Holton, H. Dobbek, P.D. Adams, U. Bergmann, N.K. Sauter, A. Zouni, J. Messinger, J. Yano, V.K. Yachandra, Structures of the Intermediates of Kok's Photosynthetic Water Oxidation Clock, Nature 563 (7731) (2018) 421–425, https://doi.org/10.1038/s41586-018-0681-2.
[3] M. Suga, F. Akita, K. Yamashita, Y. Nakajima, G. Ueno, H. Li, T. Yamane, K. Hirata, Y. Umena, S. Yonekura, L.-J. Yu, H. Murakami, T. Nomura, T. Kimura, M. Kubo, S. Baba, T. Kumasaka, K. Tono, M. Yabashi, H. Isobe, K. Yamaguchi, M. Yamamoto, H. Ago, J.-R. Shen, An Oxyl/Oxo Mechanism for Oxygen-Oxygen Coupling in PSII Revealed by an x-Ray Free-Electron Laser, Science 366 (6463) (2019) 334–338, https://doi.org/10.1126/science.aax6998.
[4] Y. Umena, K. Kawakami, J.-R. Shen, N. Kamiya, Crystal Structure of Oxygen-Evolving Photosystem II at a Resolution of 1.9 Å, Nature 473 (7345) (2011) 55–60, https://doi.org/10.1038/nature09913.
[5] A. Boussac, J.L. Zimmermann, A.W. Rutherford, EPR Signals from Modified Charge Accumulation States of the Oxygen Evolving Enzyme in Ca^{2+}-Deficient Photosystem II, Biochemistry 28 (23) (1989) 8984–8989, https://doi.org/10.1021/bi00449a005.
[6] M.J. Latimer, V.J. DeRose, V.K. Yachandra, K. Sauer, M.P. Klein, Structural Effects of Calcium Depletion on the Manganese Cluster of Photosystem II: Determination by X-Ray Absorption Spectroscopy, J. Phys. Chem. B 102 (1998) 8257–8265.
[7] D.F. Ghanotakis, G.T. Babcock, C.F. Yocum, Calcium Reconstitutes High Rates of Oxygen Evolution in Polypeptide Depleted Photosystem II Preparations, FEBS Lett. 167 (1) (1984) 127–130, https://doi.org/10.1016/0014-5793(84)80846-7.
[8] A. Boussac, A.W. Rutherford, Nature of the Inhibition of the Oxygen-Evolving Enzyme of Photosystem II Induced by Sodium Chloride Washing and Reversed by the Addition of $Calcium^{2+}$ or $Strontium^{2+}$, Biochemistry 27 (9) (1988) 3476–3483, https://doi.org/10.1021/bi00409a052.
[9] A. Boussac, F. Rappaport, P. Carrier, J.-M. Verbavatz, R. Gobin, D. Kirilovsky, A. W. Rutherford, M. Sugiura, Biosynthetic Ca^{2+}/Sr^{2+} Exchange in the Photosystem II Oxygen-Evolving Enzyme of *Thermosynechococcus Elongatus*, J. Biol. Chem. 279 (22) (2004) 22809–22819, https://doi.org/10.1074/jbc.M401677200.
[10] C.J. Kim, R.J. Debus, Evidence from FTIR Difference Spectroscopy That a Substrate H_2O Molecule for O_2 Formation in Photosystem II Is Provided by the Ca Ion of the Catalytic Mn_4CaO_5 Cluster, Biochemistry 56 (20) (2017) 2558–2570, https://doi.org/10.1021/acs.biochem.6b0127810.1021/acs.biochem.6b01278.s001.
[11] K. Saito, M. Mandal, H. Ishikita, Energetics of Ionized Water Molecules in the H-Bond Network near the Ca^{2+} and Cl^- Binding Sites in Photosystem II, Biochemistry 59 (35) (2020) 3216–3224, https://doi.org/10.1021/acs.biochem.0c0017710.1021/acs.biochem.0c00177.s00110.1021/acs.biochem.0c00177.s002.
[12] F.H.M. Koua, Y. Umena, K. Kawakami, J.-R. Shen, Structure of Sr-Substituted Photosystem II at 2.1 Å Resolution and Its Implications in the Mechanism of Water Oxidation, Proc. Natl. Acad. Sci. U.S.A 110 (10) (2013) 3889–3894, https://doi.org/10.1073/pnas.1219922110.
[13] L. Vogt, M.Z. Ertem, R. Pal, G.W. Brudvig, V.S. Batista, Computational Insights on Crystal Structures of the Oxygen-Evolving Complex of Photosystem II with Either Ca^{2+} or Ca^{2+} Substituted by Sr^{2+}, Biochemistry 54 (3) (2015) 820–825, https://doi.org/10.1021/bi5011706.
[14] M. Retegan, V. Krewald, F. Mamedov, F. Neese, W. Lubitz, N. Cox, D.A. Pantazis, A Five-Coordinate Mn(IV) Intermediate in Biological Water Oxidation: Spectroscopic Signature and a Pivot Mechanism for Water Binding, Chem. Sci. 7 (1) (2015) 72–84, https://doi.org/10.1039/C5SC03124A.
[15] M. Askerka, G.W. Brudvig, V.S. Batista, The O_2-Evolving Complex of Photosystem II: Recent Insights from Quantum Mechanics/Molecular Mechanics (QM/MM), Extended X-Ray Absorption Fine Structure (EXAFS), and Femtosecond X-Ray Crystallography Data, Acc. Chem. Res. 50 (1) (2017) 41–48, https://doi.org/10.1021/acs.accounts.6b00405.
[16] D.J. Vinyard, S. Khan, M. Askerka, V.S. Batista, G.W. Brudvig, Energetics of the S_2 State Spin Isomers of the Oxygen-Evolving Complex of Photosystem II, J. Phys. Chem. B 121 (5) (2017) 1020–1025, https://doi.org/10.1021/acs.jpcb.7b0011010.1021/acs.jpcb.7b00110.s001.
[17] A. Boussac, I. Ugur, A. Marion, M. Sugiura, V.R.I. Kaila, A.W. Rutherford, The Low Spin - High Spin Equilibrium in the S_2-State of the Water Oxidizing Enzyme, Biochim. Biophys. Acta, Bioenerg. 1859 (5) (2018) 342–356, https://doi.org/10.1016/j.bbabio.2018.02.010.
[18] J.L. Zimmermann, A.W. Rutherford, Electron Paramagnetic Resonance Properties of the S_2 State of the Oxygen-Evolving Complex of Photosystem II, Biochemistry 25 (16) (1986) 4609–4615, https://doi.org/10.1021/bi00364a023.
[19] D.A. Pantazis, W. Ames, N. Cox, W. Lubitz, F. Neese, Two Interconvertible Structures That Explain the Spectroscopic Properties of the Oxygen-evolving Complex of Photosystem II in the S_2 State, Angew. Chem. 51 (39) (2012) 9935–9940, https://doi.org/10.1002/anie.201204705.
[20] W. Ames, D.A. Pantazis, V. Krewald, N. Cox, J. Messinger, W. Lubitz, F. Neese, Theoretical Evaluation of Structural Models of the S_2 State in the Oxygen Evolving Complex of Photosystem II: Protonation States and Magnetic Interactions, J. Am. Chem. Soc. 133 (49) (2011) 19743–19757, https://doi.org/10.1021/ja2041805.
[21] T.A. Corry, P.J. O'Malley, Proton Isomers Rationalize the High- and Low-Spin Forms of the S_2 State Intermediate in the Water-Oxidizing Reaction of Photosystem II, J. Phys. Chem. Lett. 10 (17) (2019) 5226–5230, https://doi.org/10.1021/acs.jpclett.9b0137210.1021/acs.jpclett.9b01372.s001.
[22] T.A. Corry, P.J. O'Malley, Molecular Identification of a High-Spin Deprotonated Intermediate during the S_2 to S_3 Transition of Nature's Water-Oxidizing Complex, J. Am. Chem. Soc. 142 (23) (2020) 10240–10243, https://doi.org/10.1021/jacs.0c0135110.1021/jacs.0c01351.s001.
[23] M. Amin, D. Kaur, K.R. Yang, J. Wang, Z. Mohamed, G.W. Brudvig, M.R. Gunner, V. Batista, Thermodynamics of the S_2 to S_3 State Transition of the Oxygen-Evolving Complex of Photosystem II, Phys. Chem. Chem. Phys. 21 (37) (2019) 20840–20848, https://doi.org/10.1039/c9cp02308a.
[24] D. Kaur, W. Szejgis, J. Mao, M. Amin, K.M. Reiss, M. Askerka, X. Cai, U. Khaniya, Y. Zhang, G.W. Brudvig, V.S. Batista, M.R. Gunner, Relative Stability of the S_2 Isomers of the Oxygen Evolving Complex of Photosystem II, Photosyn. Res. 141 (3) (2019) 331–341, https://doi.org/10.1007/s11120-019-00637-6.

[25] D. Narzi, D. Bovi, L. Guidoni, Pathway for Mn-Cluster Oxidation by Tyrosine-Z in the S_2 State of Photosystem II, Proc. Natl. Acad. Sci. U.S.A 111 (24) (2014) 8723–8728, https://doi.org/10.1073/pnas.1401719111.
[26] P.E.M. Siegbahn, The S_2 to S_3 Transition for Water Oxidation in PSII (Photosystem II), Revisited. *Phys Chem Chem Phys* 20 (35) (2018) 22926–22931, https://doi.org/10.1039/c8cp03720e.
[27] I. Zaharieva, H. Dau, Energetics and Kinetics of S-State Transitions Monitored by Delayed Chlorophyll Fluorescence, Front. Plant Sci. 10 (2019) 386, https://doi.org/10.3389/fpls.2019.00386.
[28] I. Zaharieva, H. Dau, M. Haumann, Sequential and Coupled Proton and Electron Transfer Events in the $S_2 \rightarrow S_3$ Transition of Photosynthetic Water Oxidation Revealed by Time-Resolved X-Ray Absorption Spectroscopy, Biochemistry 55 (50) (2016) 6996–7004, https://doi.org/10.1021/acs.biochem.6b01078.
[29] M. Pérez-Navarro, F. Neese, W. Lubitz, D.A. Pantazis, N. Cox, Recent Developments in Biological Water Oxidation, Curr. Opin. Chem. Biol. 31 (2016) 113–119, https://doi.org/10.1016/j.cbpa.2016.02.007.
[30] D. Bovi, D. Narzi, L. Guidoni, The S_2 State of the Oxygen-Evolving Complex of Photosystem II Explored by QM/MM Dynamics: Spin Surfaces and Metastable States Suggest a Reaction Path towards the S_3 State, Angew. Chem. 52 (45) (2013) 11744–11749, https://doi.org/10.1002/anie.201306667.
[31] M. Shoji, H. Isobe, K. Yamaguchi, QM/MM Study of the S_2 to S_3 Transition Reaction in the Oxygen-Evolving Complex of Photosystem II, Chem. Phys. Lett. 636 (2015) 172–179, https://doi.org/10.1016/j.cplett.2015.07.039.
[32] H. Isobe, M. Shoji, J.-R. Shen, K. Yamaguchi, Strong Coupling between the Hydrogen Bonding Environment and Redox Chemistry during the S_2 to S_3 Transition in the Oxygen-Evolving Complex of Photosystem II, J. Phys. Chem. B 119 (43) (2015) 13922–13933, https://doi.org/10.1021/acs.jpcb.5b05740.
[33] I. Ugur, A.W. Rutherford, V.R.I. Kaila, Redox-Coupled Substrate Water Reorganization in the Active Site of Photosystem II—The Role of Calcium in Substrate Water Delivery, Biochim. Biophys. Acta, Bioenerg. 1857 (6) (2016) 740–748, https://doi.org/10.1016/j.bbabio.2016.01.015.
[34] S. Grimme, Semiempirical GGA-Type Density Functional Constructed with a Long-Range Dispersion Correction, J. Comput. Chem. 27 (15) (2006) 1787–1799, https://doi.org/10.1002/(ISSN)1096-987X10.1002/jcc.v27:1510.1002/jcc.20495.
[35] A.D. Becke, Density-functional Thermochemistry. III. The Role of Exact Exchange, J. Chem. Phys. 98 (7) (1993) 5648–5652, https://doi.org/10.1063/1.464913.
[36] M. Amin, L. Vogt, W. Szejgis, S. Vassiliev, G.W. Brudvig, D. Bruce, M.R. Gunner, Proton-Coupled Electron Transfer during the S-State Transitions of the Oxygen-Evolving Complex of Photosystem II, J. Phys. Chem. B 119 (24) (2015) 7366–7377, https://doi.org/10.1021/jp510948e.
[37] Y. Song, J. Mao, M.R. Gunner, MCCE2: Improving Protein pK_a Calculations with Extensive Side Chain Rotamer Sampling, J. Comput. Chem. 30 (14) (2009) 2231–2247, https://doi.org/10.1002/jcc.21222.
[38] C. Li, Z. Jia, A. Chakravorty, S. Pahari, Y. Peng, S. Basu, M. Koirala, S.K. Panday, M. Petukh, L. Li, E. Alexov, DelPhi Suite: New Developments and Review of Functionalities, J. Comput. Chem. 40 (28) (2019) 2502–2508, https://doi.org/10.1002/jcc.v40.2810.1002/jcc.26006.
[39] K. Saito, M. Nakagawa, M. Mandal, H. Ishikita, Role of Redox-Inactive Metals in Controlling the Redox Potential of Heterometallic Manganese-Oxido Clusters, Photosynth. Res. 148 (3) (2021) 153–159, https://doi.org/10.1007/s11120-021-00846-y.
[40] K. Saito, M. Nakagawa, H. Ishikita, pKa of the Ligand Water Molecules in the Oxygen-Evolving Mn_4CaO_5 Cluster in Photosystem II, Commun Chem 3 (1) (2020) 1–7, https://doi.org/10.1038/s42004-020-00336-7.
[41] M. Askerka, J. Wang, D.J. Vinyard, G.W. Brudvig, V.S. Batista, S_3 State of the O_2-Evolving Complex of Photosystem II: Insights from QM/MM, EXAFS, and Femtosecond X-Ray Diffraction, Biochemistry 55 (7) (2016) 981–984, https://doi.org/10.1021/acs.biochem.6b0004110.1021/acs.biochem.6b00041.s00210.1021/acs.biochem.6b00041.s003.
[42] M. Askerka, D.J. Vinyard, G.W. Brudvig, V.S. Batista, NH_3 Binding to the S_2 State of the O_2-Evolving Complex of Photosystem II: Analogue to H_2O Binding during the $S_2 \rightarrow S_3$ Transition, Biochemistry 54 (38) (2015) 5783–5786, https://doi.org/10.1021/acs.biochem.5b00974.
[43] J. Wang, M. Askerka, G.W. Brudvig, V.S. Batista, Crystallographic Data Support the Carousel Mechanism of Water Supply to the Oxygen-Evolving Complex of Photosystem II, ACS Energy Lett. 2 (10) (2017) 2299–2306, https://doi.org/10.1021/acsenergylett.7b0075010.1021/acsenergylett.7b00750.s001.
[44] C.J. Kim, R.J. Debus, One of the Substrate Waters for O_2 Formation in Photosystem II Is Provided by the Water-Splitting Mn_4CaO_5 Cluster's Ca^{2+} Ion, Biochemistry 58 (29) (2019) 3185–3192, https://doi.org/10.1021/acs.biochem.9b00418.
[45] K. Kawashima, T. Takaoka, H. Kimura, K. Saito, H. Ishikita, O_2 Evolution and Recovery of the Water-Oxidizing Enzyme, Nat. Commun. 9 (1) (2018) 1247, https://doi.org/10.1038/s41467-018-03545-w.
[46] K.R. Yang, K.V. Lakshmi, G.W. Brudvig, V.S. Batista, Is Deprotonation of the Oxygen-Evolving Complex of Photosystem II during the $S_1 \rightarrow S_2$ Transition Suppressed by Proton Quantum Delocalization? J. Am. Chem. Soc. 143 (22) (2021) 8324–8332, https://doi.org/10.1021/jacs.1c0063310.1021/jacs.1c00633.s00110.1021/jacs.1c00633.s00210.1021/jacs.1c00633.s00310.1021/jacs.1c00633.s004.
[47] H. Kuroda, K. Kawashima, K. Ueda, T. Ikeda, K. Saito, R. Ninomiya, C. Hida, Y. Takahashi, H. Ishikita, Proton Transfer Pathway from the Oxygen-Evolving Complex in Photosystem II Substantiated by Extensive Mutagenesis, Biochim. Biophys. Acta, Bioenerg. 1862 (1) (2021) 148329, https://doi.org/10.1016/j.bbabio.2020.148329.
[48] M. Ibrahim, T. Fransson, R. Chatterjee, M.H. Cheah, R. Hussein, L. Lassalle, K. D. Sutherlin, I.D. Young, F.D. Fuller, S. Gul, I.-S. Kim, P.S. Simon, C. de Lichtenberg, P. Chernev, I. Bogacz, C.C. Pham, A.M. Orville, N. Saichek, T. Northen, A. Batyuk, S. Carbajo, R. Alonso-Mori, K. Tono, S. Owada, A. Bhowmick, R. Bolotovsky, D. Mendez, N.W. Moriarty, J.M. Holton, H. Dobbek, A.S. Brewster, P.D. Adams, N.K. Sauter, U. Bergmann, A. Zouni, J. Messinger, J. Kern, V.K. Yachandra, J. Yano, Untangling the Sequence of Events during the $S_2 \rightarrow S_3$ Transition in Photosystem II and Implications for the Water Oxidation Mechanism, Proc. Natl. Acad. Sci. USA 117 (23) (2020) 12624–12635, https://doi.org/10.1073/pnas.2000529117.